Initial Relative-Orbit Determination using Heterogeneous TDOA

Simon Shuster
Mechanical and Aerospace Engineering
Utah State University
Logan, UT 84322
simon.shuster@aggiemail.usu.edu

Andrew J. Sinclair
Space Vehicles Directorate
Air Force Research Laboratory
Kirtland AFB, NM 87117
505-846-2152
afrl.rvsv@kirtland.af.mil

T. Alan Lovell
Space Vehicles Directorate
Air Force Research Laboratory
Kirtland AFB, NM 87117
505-846-2152
afrl.rvsv@kirtland.af.mil

Abstract—**This paper presents a solution for the initial orbit determination of a space-based RF transmitter using time-difference-of-arrival (TDOA) measurements obtained from space-based receivers in known orbits. Orbit determination requires six independent TDOA measurements spread over time. The TDOA measurement can be expressed as a quadratic equation for the instantaneous transmitter position. The orbital motion of the transmitter is linearized relative to a reference orbit, which allows the TDOA measurement to be transformed to a quadratic equation for the relative position and velocity components at a chosen initial time. The system of six quadratic equations are solved using homotopy continuation.**

TABLE OF CONTENTS

1. INTRODUCTION

Time-difference-of-arrival (TDOA) measurements, using ground or space-based receivers, have been widely studied for the geolocation of a ground-based radio frequency (RF) transmitter [1–10]. This paper investigates the novel problem of initial relative-orbit determination (IROD) of a space-based RF transmitter via TDOA. The use of a satellite formation to determine the unknown orbit of an RF transmitter has a wide array of military and civilian applications, including space situational awareness. Unlike the Global Positioning System (GPS) which uses a highly structured and well defined signal, the goal here is to be able to collect measurements that require little a priori information about the signal. One approach is to use TDOA measurements. The TDOA measurement is formed by comparing the signal received by two non-collocated receivers. By knowing the speed of the signal's propagation, the TDOA measurement can be related to the difference in the ranges from the transmitter to the two receivers. The analytic expression for this range difference places the transmitter on one sheet of a two-sheeted hyperboloid with the two receivers located at the foci. Because the orbit of the transmitter is described by six state variables, determining this orbit of the transmitter requires six TDOA measurements over time, combined with a model for the relative motion of the transmitter with respect to the receivers.

This paper investigates IROD via a linearized dynamics model referred to as the DeVries equations [11], which in the special case of a circular reference orbit simplify to the Clohessy-Wiltshire equations [12]. One measurement approach is to use a formation of four receivers that can instantaneously collect three independent TDOA measurements. Using three TDOA measurements, the instantaneous transmitter position can be calculated using solutions identical to those developed previously for fixed, ground-based transmitters [1, 2, 7, 10]. From solutions for the position at two instants in time, the state-transition matrix can be used to solve for the relative velocity, and thus the relative orbit of the transmitter.

Alternatively, a formation of only two or three receivers can be considered, which cannot collect enough independent TDOA measurements at a single instant to solve for the transmitter position. Each measurement can be expressed as a quadratic function of the transmitter's instantaneous position components. Using the linear dynamics model, these equations can be rewritten as quadratic functions of the six initial position and velocity components. Six TDOA measurements collected at two or more instants in time, with no more than three measurements at any individual instant, produce a system of six coupled quadratic equations for six unknowns. The remainder of the paper is organized as follows. Section 2 describes the dynamic and measurement models. Section 3 presents a solution procedure when four receivers are available, and section 4 presents a more general solution procedure that applies to two or three receivers. Section 5 analyzes the covariance and bias in the IROD solution. Section 6 presents two examples with Monte Carlo simulations. Finally some conclusions are given in section 7.

2. DYNAMIC AND MEASUREMENT MODELS

The motion of an orbiting RF transmitter can be described relative to a reference point following a Keplerian orbit. The position of the transmitter relative to the reference point is defined as $\boldsymbol{r}$. The vector $\boldsymbol{r}$ has components $[x\ y\ z]^\mathsf{T}$ in a local-vertical/local-horizontal (LVLH) reference frame attached to the reference point with the x component pointing in the radial direction, the y component pointing in the transverse direction, and the z component pointing in the direction of the reference orbit's angular momentum. The relative velocity is defined as $\boldsymbol{v}$ with LVLH components $[\dot{x}\ \dot{y}\ \dot{z}]^\mathsf{T}$. Assuming that the transmitter follows a Keplerian orbit and that the transmitter is in close proximity to the reference point, the transmitter's motion can be described by

978-1-5090-1613-6/17/31.00 ©2017 IEEE

the DeVries equations [11].

$$
\begin{aligned}
\ddot{x} - \dot{f}^2\left(1 + 2\frac{r}{p}\right)x - 2\dot{f}\left(\dot{y} - \frac{\dot{r}}{r}y\right) &= 0 \\
\ddot{y} + 2\dot{f}\left(\dot{x} - \frac{\dot{r}}{r}x\right) - \dot{f}^2\left(1 - \frac{r}{p}\right)y &= 0 \\
\ddot{z} + \frac{r}{p}\dot{f}^2 z &= 0
\end{aligned} \tag{1}
$$

Here, r is the reference orbit's radius, p is the reference orbit's semilatus rectum, and f is the reference point's true anomaly. Several forms for solutions to these equations have been presented [13–15]. The state vector $\boldsymbol{x} = [x\ y\ z\ \dot{x}\ \dot{y}\ \dot{z}]^\mathsf{T}$ can be defined, and the solution is expressed here in terms of the state-transition matrix, $\boldsymbol{\Phi}$.

$$
\boldsymbol{x}_k = \boldsymbol{\Phi}(t_k, t_0)\boldsymbol{x}_0 \tag{2}
$$

For later convenience, the state-transition matrix can be partitioned into four 3×3 submatrices.

$$
\boldsymbol{\Phi}(t_k, t_0) = \begin{bmatrix} \boldsymbol{\Phi}_{rr}(t_k, t_0) & \boldsymbol{\Phi}_{rv}(t_k, t_0) \\ \boldsymbol{\Phi}_{vr}(t_k, t_0) & \boldsymbol{\Phi}_{vv}(t_k, t_0) \end{bmatrix} \tag{3}
$$

Assume the TDOA measurement at the epoch t_k is given by $\Delta t_k = t_{2,k} - t_{1,k}$. Here, the subscripts 1 and 2 refer to the two receivers involved in defining the kth TDOA measurement, and these labels do not necessarily identify the same physical receivers across other TDOA measurements. Additionally, up to three TDOA measurements can be allowed to have identical epoch times. The range difference, $\Delta\rho_k$, between the receivers is then given by the following, with all positions expressed in the LVLH coordinate frame.

$$
\begin{aligned}
\Delta\rho_k &= c\Delta t_k = \rho_{2,k} - \rho_{1,k} \\
&= \left[(x_k - x_{2,k})^2 + (y_k - y_{2,k})^2 + (z_k - z_{2,k})^2\right]^{\frac{1}{2}} \\
&\quad - \left[(x_k - x_{1,k})^2 + (y_k - y_{1,k})^2 + (z_k - z_{1,k})^2\right]^{\frac{1}{2}}
\end{aligned} \tag{4}
$$

Here, $x_{1,k}$, $y_{1,k}$, and $z_{1,k}$ are the known position components of the first receiver, $x_{2,k}$, $y_{2,k}$, and $z_{2,k}$ are the known position components of the second receiver, and x_k, y_k, and z_k are the unknown position components of the transmitter. Whereas the TDOA measurement is actually a time difference with units of time, in the subsequent, the term TDOA will be used to refer to the range difference with units of length.

Through algebraic manipulation, Eq. (4) can be transformed into a second-order polynomial for the instantaneous transmitter position components [10].

$$
\begin{aligned}
& x_k^2\left((x_{1,k} - x_{2,k})^2 - \Delta\rho_k^2\right) \\
& + 2x_k y_k (x_{1,k} - x_{2,k})(y_{1,k} - y_{2,k}) \\
& + 2x_k z_k (x_{1,k} - x_{2,k})(z_{1,k} - z_{2,k}) \\
& + y_k^2\left((y_{1,k} - y_{2,k})^2 - \Delta\rho_k^2\right) \\
& + 2y_k z_k (y_{1,k} - y_{2,k})(z_{1,k} - z_{2,k}) \\
& + z_k^2\left((z_{1,k} - z_{2,k})^2 - \Delta\rho_k^2\right) \\
& + x_k\left((x_{1,k} - x_{2,k})\left(K_{2,k} - K_{1,k} - \Delta\rho_k^2\right) + 2\Delta\rho_k^2 x_{1,k}\right) \\
& + y_k\left((y_{1,k} - y_{2,k})\left(K_{2,k} - K_{1,k} - \Delta\rho_k^2\right) + 2\Delta\rho_k^2 y_{1,k}\right) \\
& + z_k\left((z_{1,k} - z_{2,k})\left(K_{2,k} - K_{1,k} - \Delta\rho_k^2\right) + 2\Delta\rho_k^2 z_{1,k}\right) \\
& + \frac{1}{4}\left(K_{2,k} - K_{1,k} - \Delta\rho_k^2\right)^2 - \Delta\rho_k^2 K_{1,k} = 0
\end{aligned} \tag{5}
$$

Here, $K_{i,k} = x_{i,k}^2 + y_{i,k}^2 + z_{i,k}^2$, which is actually the square of the distance from the ith receiver to the reference point at the kth epoch.

3. Four-Receiver Solution

With four receivers able to collect three independent TDOA measurements at the same epoch, a special solution procedure is possible. This procedure first solves the TDOA equations for relative positions at two different epochs, and then uses the dynamic model to solve for the relative velocity at one of the two epochs. Label the four receivers as A, B, C, and D. At each epoch, three instantiations of Eq. (5) can be written by taking three pairs of combinations of A, B, C, and D, such that each receiver is included in at least one pair. This represents three quadratic equations for the transmitter position components at the epoch. Solution for these position components can be performed similar to previous methods developed for TDOA geolocation (see e.g. [1, 2, 7, 10]).

Collecting the TDOA measurements at epochs t_1 and t_2 allows solution for the relative positions at each epoch, $\boldsymbol{r}_1$ and $\boldsymbol{r}_2$. This reduces the problem to a two-point boundary value problem to solve for the velocity at t_1.

$$
\boldsymbol{v}_1 = \boldsymbol{\Phi}_{rv}^{-1}(t_2, t_1)\left(\boldsymbol{r}_2 - \boldsymbol{\Phi}_{rr}(t_2, t_1)\boldsymbol{r}_1\right) \tag{6}
$$

Using the solution for the position and velocity at t_1, the state at the initial time can be computed.

$$
\boldsymbol{x}_0 = \boldsymbol{\Phi}(t_0, t_1)\boldsymbol{x}_1 \tag{7}
$$

4. Two or Three-Receiver Solution

With less than four receivers, the sequential solution for the relative position first and the relative velocity second is not possible. Instead, the dynamic model must be substituted into Eq. (5) to produce a quadratic equation in the six initial states. Collection of six independent TDOA measurements (possibly by two receivers at six epochs or by three receivers at three epochs) produces a system of six quadratic equations for the six unknown initial states. This system has up to 64 finite solutions, for which disambiguation is required. The disambiguation could be performed using external information about the transmitter's orbit, by using an additional TDOA measurement, or by considering the domain of applicability of the linear dynamics model used in developing the solutions. However, the disambiguation process is not further addressed here.

Previous work for TDOA geolocation suggested solving the system of three quadratic equations using resultant methods [7, 10]. Preliminary investigation in applying the Macaulay resultant method to the IROD system of six quadratic equations (the same approach used for three quadratic equations in [10]) demonstrated large numerical errors. As an alternative, the solutions were obtained here using Bertini [16], a homotopy continuation method.

5. SOLUTION ACCURACY

Following previous studies [10], the IROD accuracy can be evaluated by Taylor expansion. The transmitter-initial-state covariance and bias are developed considering uncertainty in both the TDOA measurements and receiver locations. Another error source is dynamic modeling error due to differences between the linearized solution in Eq. (2) and the true orbital motion of the transmitter. This dynamic modeling error increases as the separation between the transmitter and the reference point increases and as the propagation time increases. However, this dynamic modeling error is not further considered here.

Error Covariance

Define the following vectors for the TDOA measurements and the jth receiver's position at the kth measurement.

$$\Delta\boldsymbol{\rho} = \begin{bmatrix} \Delta\rho_1 \\ \Delta\rho_2 \\ \Delta\rho_3 \\ \Delta\rho_4 \\ \Delta\rho_5 \\ \Delta\rho_6 \end{bmatrix} \qquad \boldsymbol{r}_{j,k} = \begin{bmatrix} x_{j,k} \\ y_{j,k} \\ z_{j,k} \end{bmatrix} \tag{8}$$

Using Eqs. (4) and (2), the TDOA measurements can be defined as a vector function of the transmitter initial state and the receiver locations at each measurement epoch.

$$\Delta\boldsymbol{\rho} = \boldsymbol{h}\left(\boldsymbol{x}_0, \boldsymbol{r}_{1,1}, \boldsymbol{r}_{2,1}, \ldots, \boldsymbol{r}_{1,6}, \boldsymbol{r}_{2,6}\right) \tag{9}$$

Of course, the kth element of $\Delta\boldsymbol{\rho}$ is a function of only $\boldsymbol{x}_0$, $\boldsymbol{r}_{1,k}$, and $\boldsymbol{r}_{2,k}$.

Deviations in the measurements and receiver locations will produce uncertainties in the transmitter location. The measured values for TDOAs and receiver locations can be written as the true values plus deviations.

$$\Delta\tilde{\boldsymbol{\rho}} = \Delta\boldsymbol{\rho} + \delta\Delta\boldsymbol{\rho} \qquad \tilde{\boldsymbol{r}}_{j,k} = \boldsymbol{r}_{j,k} + \delta\boldsymbol{r}_{j,k} \tag{10}$$

The resulting estimated value for the transmitter initial state can be written as the true value plus a deviation.

$$\hat{\boldsymbol{x}}_0 = \boldsymbol{x}_0 + \delta\boldsymbol{x}_0 \tag{11}$$

Here, $\tilde{()}$ indicates a measured quantity, $\hat{()}$ indicates an estimated quantity, and $\delta()$ represents a deviation.

Assuming small deviations, the deviations must satisfy the following relation.

$$\delta\Delta\boldsymbol{\rho} = \boldsymbol{H}_0\delta\boldsymbol{x}_0 + \sum_{j=1}^{2}\sum_{k=1}^{6}\boldsymbol{H}_{j,k}\delta\boldsymbol{r}_{j,k} \tag{12}$$

$$\boldsymbol{H}_0 \equiv \frac{\partial\boldsymbol{h}}{\partial\boldsymbol{x}_0} \qquad \boldsymbol{H}_{j,k} \equiv \frac{\partial\boldsymbol{h}}{\partial\boldsymbol{r}_{j,k}} \tag{13}$$

Note that $\boldsymbol{H}_0$ and $\boldsymbol{H}_{j,k}$ are functions of the transmitter and receiver locations. Of course, only the kth row of $\boldsymbol{H}_{j,k}$ is nonzero. Assuming $\boldsymbol{H}_0$ is invertible, the deviation in the transmitter initial state can be found.

$$\delta\boldsymbol{x}_0 = \boldsymbol{H}_0^{-1}\left(\delta\Delta\boldsymbol{\rho} - \sum_{j=1}^{2}\sum_{k=1}^{6}\boldsymbol{H}_{j,k}\delta\boldsymbol{r}_{j,k}\right) \tag{14}$$

Next, the covariances in the transmitter initial state, TDOA measurements, and receiver locations are defined.

$$\boldsymbol{P}_0 \equiv \mathrm{E}\left\{\delta\boldsymbol{x}_0\delta\boldsymbol{x}_0^{\mathsf{T}}\right\} \tag{15}$$

$$\boldsymbol{P}_{\Delta\rho} \equiv \mathrm{E}\left\{\delta\Delta\boldsymbol{\rho}_T\delta\Delta\boldsymbol{\rho}_T^{\mathsf{T}}\right\} \qquad \boldsymbol{P}_{j,k} \equiv \mathrm{E}\left\{\delta\boldsymbol{r}_{j,k}\delta\boldsymbol{r}_{j,k}^{\mathsf{T}}\right\} \tag{16}$$

Assuming the deviations in the TDOA measurements and receiver locations are uncorrelated, the transmitter-initial-state covariance is given by the following.

$$\boldsymbol{P}_0 = \boldsymbol{H}_0^{-1}\left(\boldsymbol{P}_{\Delta\rho} + \sum_{j=1}^{2}\sum_{k=1}^{3}\boldsymbol{H}_{j,k}\boldsymbol{P}_{j,k}\boldsymbol{H}_{j,k}^{\mathsf{T}}\right)\boldsymbol{H}_0^{-\mathsf{T}} \tag{17}$$

Clearly, the transmitter-initial-state covariance is a function of the TDOA measurement covariance and the reciever-location covariance. As mentioned, $\boldsymbol{H}_0$ and $\boldsymbol{H}_{j,k}$, and therefore $\boldsymbol{P}_0$, are functions of the true transmitter initial state and receiver locations. This indicates how the localization accuracy is a function of the measurement geometry, even if intuitive insight into this dependency is difficult to extract from Eq. (17). For later convenience, the covariance matrix can be partitioned into 3×3 submatrices.

$$\boldsymbol{P}_0 = \begin{bmatrix} \boldsymbol{P}_{rr} & \boldsymbol{P}_{rv} \\ \boldsymbol{P}_{rv} & \boldsymbol{P}_{vv} \end{bmatrix} \tag{18}$$

Error Bias

Taking the expected value of Eq. (14) indicates that zero-mean errors in the TDOA measurements and receiver locations will produce an unbiased solution for the transmitter location. However, a more accurate prediction of the solution bias can be obtained from a second-order expansion of Eq. (9). The second-order variation of the kth measurement with respect to $\boldsymbol{x}_0$, $\boldsymbol{r}_{1,k}$, and $\boldsymbol{r}_{2,k}$ is shown below.

$$\begin{aligned}\delta\Delta\rho_k =& \frac{\partial h_k}{\partial \boldsymbol{x}_0}\delta\boldsymbol{x}_0 + \frac{\partial h_k}{\partial \boldsymbol{r}_{1,k}}\delta\boldsymbol{r}_{1,k} + \frac{\partial h_k}{\partial \boldsymbol{r}_{2,k}}\delta\boldsymbol{r}_{2,k} \\ &+ \frac{1}{2}\delta\boldsymbol{x}_0^\mathsf{T}\frac{\partial^2 h_k}{\partial \boldsymbol{x}_0^2}\delta\boldsymbol{x}_0 + \delta\boldsymbol{x}_0^\mathsf{T}\frac{\partial^2 h_k}{\partial \boldsymbol{x}_0\partial\boldsymbol{r}_{1,k}}\delta\boldsymbol{r}_{1,k} \\ &+ \delta\boldsymbol{x}_0^\mathsf{T}\frac{\partial^2 h_k}{\partial \boldsymbol{x}_0\partial\boldsymbol{r}_{2,k}}\delta\boldsymbol{r}_{2,k} + \frac{1}{2}\delta\boldsymbol{r}_{1,k}^\mathsf{T}\frac{\partial^2 h_k}{\partial \boldsymbol{r}_{1,k}^2}\delta\boldsymbol{r}_{1,k} \\ &+ \delta\boldsymbol{r}_{1,k}^\mathsf{T}\frac{\partial^2 h_k}{\partial \boldsymbol{r}_{1,k}\partial\boldsymbol{r}_{2,k}}\delta\boldsymbol{r}_{2,k} + \frac{1}{2}\delta\boldsymbol{r}_{2,k}^\mathsf{T}\frac{\partial^2 h_k}{\partial \boldsymbol{r}_{2,k}^2}\delta\boldsymbol{r}_{2,k} \end{aligned} \tag{19}$$

$$\begin{aligned}=& \left(\frac{\partial h_k}{\partial \boldsymbol{x}_0} + \delta\boldsymbol{r}_{1,k}^\mathsf{T}\frac{\partial^2 h_k}{\partial \boldsymbol{r}_{1,k}\partial\boldsymbol{x}_0} + \delta\boldsymbol{r}_{2,k}^\mathsf{T}\frac{\partial^2 h_k}{\partial \boldsymbol{r}_{2,k}\partial\boldsymbol{x}_0}\right)\delta\boldsymbol{x}_0 \\ &+ \frac{\partial h_k}{\partial \boldsymbol{r}_{1,k}}\delta\boldsymbol{r}_{1,k} + \frac{\partial h_k}{\partial \boldsymbol{r}_{2,k}}\delta\boldsymbol{r}_{2,k} + \frac{1}{2}\delta\boldsymbol{x}_0^\mathsf{T}\frac{\partial^2 h_k}{\partial \boldsymbol{x}_0^2}\delta\boldsymbol{x}_0 \\ &+ \frac{1}{2}\delta\boldsymbol{r}_{1,k}^\mathsf{T}\frac{\partial^2 h_k}{\partial \boldsymbol{r}_{1,k}^2}\delta\boldsymbol{r}_{1,k} + \delta\boldsymbol{r}_{1,k}^\mathsf{T}\frac{\partial^2 h_k}{\partial \boldsymbol{r}_{1,k}\partial\boldsymbol{r}_{2,k}}\delta\boldsymbol{r}_{2,k} \\ &+ \frac{1}{2}\delta\boldsymbol{r}_{2,k}^\mathsf{T}\frac{\partial^2 h_k}{\partial \boldsymbol{r}_{2,k}^2}\delta\boldsymbol{r}_{2,k}\end{aligned}$$

The expansions for the three measurements can be grouped into a matrix-vector form, and terms linear in $\delta\boldsymbol{x}_0$ are collected.

$$(\boldsymbol{H}_0 + \boldsymbol{C})\,\delta\boldsymbol{x}_0 = \boldsymbol{d}_1 + \boldsymbol{d}_2 \tag{20}$$

$$\boldsymbol{C} = \begin{bmatrix} \delta\boldsymbol{r}_{1,1}^\mathsf{T}\frac{\partial^2 h_1}{\partial\boldsymbol{r}_{1,1}\partial\boldsymbol{x}_0} + \delta\boldsymbol{r}_{2,1}^\mathsf{T}\frac{\partial^2 h_1}{\partial\boldsymbol{r}_{2,1}\partial\boldsymbol{x}_0} \\ \vdots \\ \delta\boldsymbol{r}_{1,6}^\mathsf{T}\frac{\partial^2 h_6}{\partial\boldsymbol{r}_{1,6}\partial\boldsymbol{x}_0} + \delta\boldsymbol{r}_{2,6}^\mathsf{T}\frac{\partial^2 h_6}{\partial\boldsymbol{r}_{2,6}\partial\boldsymbol{x}_0} \end{bmatrix} \tag{21}$$

$$\boldsymbol{d}_1 = \begin{bmatrix} \delta\Delta\rho_1 - \frac{\partial h_1}{\partial\boldsymbol{r}_{1,1}}\delta\boldsymbol{r}_{1,1} - \frac{\partial h_1}{\partial\boldsymbol{r}_{2,1}}\delta\boldsymbol{r}_{2,1} \\ \vdots \\ \delta\Delta\rho_6 - \frac{\partial h_6}{\partial\boldsymbol{r}_{1,6}}\delta\boldsymbol{r}_{1,6} - \frac{\partial h_6}{\partial\boldsymbol{r}_{2,6}}\delta\boldsymbol{r}_{2,6} \end{bmatrix} \tag{22}$$

$$\boldsymbol{d}_2 = -\begin{bmatrix} \frac{1}{2}\delta\boldsymbol{x}_0^\mathsf{T}\frac{\partial^2 h_1}{\partial\boldsymbol{x}_0^2}\delta\boldsymbol{x}_0 + \frac{1}{2}\delta\boldsymbol{r}_{1,1}^\mathsf{T}\frac{\partial^2 h_1}{\partial\boldsymbol{r}_{1,1}^2}\delta\boldsymbol{r}_{1,1} \\ +\delta\boldsymbol{r}_{1,1}^\mathsf{T}\frac{\partial^2 h_1}{\partial\boldsymbol{r}_{1,1}\partial\boldsymbol{r}_{2,1}}\delta\boldsymbol{r}_{2,1} + \frac{1}{2}\delta\boldsymbol{r}_{2,1}^\mathsf{T}\frac{\partial^2 h_1}{\partial\boldsymbol{r}_{2,1}^2}\delta\boldsymbol{r}_{2,1} \\ \vdots \\ \frac{1}{2}\delta\boldsymbol{x}_0^\mathsf{T}\frac{\partial^2 h_6}{\partial\boldsymbol{x}_0^2}\delta\boldsymbol{x}_0 + \frac{1}{2}\delta\boldsymbol{r}_{1,6}^\mathsf{T}\frac{\partial^2 h_6}{\partial\boldsymbol{r}_{1,6}^2}\delta\boldsymbol{r}_{1,6} \\ +\delta\boldsymbol{r}_{1,6}^\mathsf{T}\frac{\partial^2 h_6}{\partial\boldsymbol{r}_{1,6}\partial\boldsymbol{r}_{2,6}}\delta\boldsymbol{r}_{2,6} + \frac{1}{2}\delta\boldsymbol{r}_{2,6}^\mathsf{T}\frac{\partial^2 h_6}{\partial\boldsymbol{r}_{2,6}^2}\delta\boldsymbol{r}_{2,6} \end{bmatrix} \tag{23}$$

Equation (20) can be rewritten by inverting $\boldsymbol{H}_0$.

$$\left(\boldsymbol{I} + \boldsymbol{H}_0^{-1}\boldsymbol{C}\right)\delta\boldsymbol{x}_0 = \boldsymbol{H}_0^{-1}(\boldsymbol{d}_1 + \boldsymbol{d}_2) \tag{24}$$

Because the righthand side above contains terms that are linear and quadratic in the various errors, an expression for $\delta\boldsymbol{x}_0$ that is accurate to second order can be obtained by approximating the inverse of $(\boldsymbol{I} + \boldsymbol{H}_0^{-1}\boldsymbol{C})$ to first-order accuracy in the receiver-location errors.

$$\delta\boldsymbol{x}_0 = \left(\boldsymbol{I} - \boldsymbol{H}_0^{-1}\boldsymbol{C}\right)\boldsymbol{H}_0^{-1}(\boldsymbol{d}_1 + \boldsymbol{d}_2) \tag{25}$$

Again, since a second-order expression for $\delta\boldsymbol{x}_0$ is desired, the third-order terms can be discarded.

$$\delta\boldsymbol{x}_0 = \boldsymbol{H}_0^{-1}(\boldsymbol{d}_1 + \boldsymbol{d}_2) - \boldsymbol{H}_0^{-1}\boldsymbol{C}\boldsymbol{H}_0^{-1}\boldsymbol{d}_1 \tag{26}$$

For convenience in the following developments, the quantity $\boldsymbol{C}\boldsymbol{H}_0^{-1}\boldsymbol{d}_1$ is expanded below.

$$\boldsymbol{C}\boldsymbol{H}_0^{-1}\boldsymbol{d}_1 = \tag{27}$$
$$\begin{bmatrix} \delta\boldsymbol{r}_{1,1}^\mathsf{T}\frac{\partial^2 h_1}{\partial\boldsymbol{r}_{1,1}\partial\boldsymbol{x}_0}\boldsymbol{H}_0^{-1}\boldsymbol{d}_1 + \delta\boldsymbol{r}_{2,1}^\mathsf{T}\frac{\partial^2 h_1}{\partial\boldsymbol{r}_{2,1}\partial\boldsymbol{x}_0}\boldsymbol{H}_0^{-1}\boldsymbol{d}_1 \\ \vdots \\ \delta\boldsymbol{r}_{1,6}^\mathsf{T}\frac{\partial^2 h_6}{\partial\boldsymbol{r}_{1,6}\partial\boldsymbol{x}_0}\boldsymbol{H}_0^{-1}\boldsymbol{d}_1 + \delta\boldsymbol{r}_{2,6}^\mathsf{T}\frac{\partial^2 h_6}{\partial\boldsymbol{r}_{2,6}\partial\boldsymbol{x}_0}\boldsymbol{H}_0^{-1}\boldsymbol{d}_1 \end{bmatrix}$$

Next, the expected value of $\delta\boldsymbol{x}_0$ is taken, assuming the measurement errors and receiver-location errors are zero-mean and uncorrelated.

$$\boldsymbol{b}_0 \equiv \mathrm{E}\{\delta\boldsymbol{x}_0\} = \boldsymbol{H}_0^{-1}\left(\mathrm{E}\{\boldsymbol{d}_1\} + \mathrm{E}\{\boldsymbol{d}_2\} - \mathrm{E}\left\{\boldsymbol{C}\boldsymbol{H}_0^{-1}\boldsymbol{d}_1\right\}\right) \tag{28}$$

$$\mathrm{E}\{\boldsymbol{d}_1\} = \boldsymbol{0} \tag{29}$$

$$\mathrm{E}\{\boldsymbol{d}_2\} = \tag{30}$$
$$-\begin{bmatrix} \frac{1}{2}\mathrm{tr}\left(\frac{\partial^2 h_1}{\partial\boldsymbol{x}_0^2}\boldsymbol{P}_0\right) + \frac{1}{2}\mathrm{tr}\left(\frac{\partial^2 h_1}{\partial\boldsymbol{r}_{1,1}^2}\boldsymbol{P}_{1,1}\right) + \frac{1}{2}\mathrm{tr}\left(\frac{\partial^2 h_1}{\partial\boldsymbol{r}_{2,1}^2}\boldsymbol{P}_{2,1}\right) \\ \vdots \\ \frac{1}{2}\mathrm{tr}\left(\frac{\partial^2 h_6}{\partial\boldsymbol{x}_0^2}\boldsymbol{P}_0\right) + \frac{1}{2}\mathrm{tr}\left(\frac{\partial^2 h_6}{\partial\boldsymbol{r}_{1,6}^2}\boldsymbol{P}_{1,6}\right) + \frac{1}{2}\mathrm{tr}\left(\frac{\partial^2 h_6}{\partial\boldsymbol{r}_{2,6}^2}\boldsymbol{P}_{2,6}\right) \end{bmatrix}$$

$$\mathrm{E}\left\{\boldsymbol{C}\boldsymbol{H}_0^{-1}\boldsymbol{d}_1\right\} = \tag{31}$$
$$\begin{bmatrix} \mathrm{tr}\left\{-\frac{\partial^2 h_1}{\partial\boldsymbol{r}_{1,1}\partial\boldsymbol{x}_0}\boldsymbol{H}_0^{-1}\begin{bmatrix}\frac{\partial h_1}{\partial\boldsymbol{r}_{1,1}}\boldsymbol{P}_{1,1} \\ \boldsymbol{0}^\mathsf{T} \\ \boldsymbol{0}^\mathsf{T} \\ \boldsymbol{0}^\mathsf{T} \\ \boldsymbol{0}^\mathsf{T} \\ \boldsymbol{0}^\mathsf{T}\end{bmatrix}\right\} \\ +\mathrm{tr}\left\{-\frac{\partial^2 h_1}{\partial\boldsymbol{r}_{2,1}\partial\boldsymbol{x}_0}\boldsymbol{H}_0^{-1}\begin{bmatrix}\frac{\partial h_1}{\partial\boldsymbol{r}_{2,1}}\boldsymbol{P}_{2,1} \\ \boldsymbol{0}^\mathsf{T} \\ \boldsymbol{0}^\mathsf{T} \\ \boldsymbol{0}^\mathsf{T} \\ \boldsymbol{0}^\mathsf{T} \\ \boldsymbol{0}^\mathsf{T}\end{bmatrix}\right\} \\ \vdots \\ \mathrm{tr}\left\{-\frac{\partial^2 h_6}{\partial\boldsymbol{r}_{1,6}\partial\boldsymbol{x}_0}\boldsymbol{H}_0^{-1}\begin{bmatrix}\boldsymbol{0}^\mathsf{T} \\ \boldsymbol{0}^\mathsf{T} \\ \boldsymbol{0}^\mathsf{T} \\ \boldsymbol{0}^\mathsf{T} \\ \boldsymbol{0}^\mathsf{T} \\ \frac{\partial h_6}{\partial\boldsymbol{r}_{1,6}}\boldsymbol{P}_{1,6}\end{bmatrix}\right\} \\ +\mathrm{tr}\left\{-\frac{\partial^2 h_6}{\partial\boldsymbol{r}_{2,6}\partial\boldsymbol{x}_0}\boldsymbol{H}_0^{-1}\begin{bmatrix}\boldsymbol{0}^\mathsf{T} \\ \boldsymbol{0}^\mathsf{T} \\ \boldsymbol{0}^\mathsf{T} \\ \boldsymbol{0}^\mathsf{T} \\ \boldsymbol{0}^\mathsf{T} \\ \frac{\partial h_6}{\partial\boldsymbol{r}_{2,6}}\boldsymbol{P}_{2,6}\end{bmatrix}\right\} \end{bmatrix}$$

Here, $\boldsymbol{0}^\mathsf{T}$ is a 1×6 row of zeros. Note that the covariances in the receiver locations directly contribute to $\mathrm{E}\{\boldsymbol{d}_2\}$ and $\mathrm{E}\{\boldsymbol{C}\boldsymbol{H}_0^{-1}\boldsymbol{d}_1\}$, and the covariances in the receiver locations and the TDOA measurements indirectly contribute to $\mathrm{E}\{\boldsymbol{d}_2\}$ through $\boldsymbol{P}_0$.

6. Examples

Four-Receiver Example

Consider a circular reference orbit with semimajor axis of 7100 km. The initial states of four receivers and the transmitter, in units of km and km/s, are shown below.

$$\boldsymbol{x}_{A,0} = \begin{bmatrix} 0 \\ 0 \\ 0 \\ 0 \\ 0 \\ 0 \end{bmatrix} \quad \boldsymbol{x}_{B,0} = \begin{bmatrix} 0 \\ 1 \\ 0.1 \\ 0 \\ 0 \\ 0 \end{bmatrix} \quad \boldsymbol{x}_{C,0} = \begin{bmatrix} 1 \\ 0 \\ 0 \\ 0 \\ -2n \\ 0 \end{bmatrix} \tag{32}$$

$$\boldsymbol{x}_{D,0} = \begin{bmatrix} 0 \\ 0.5 \\ 1 \\ 0 \\ 0 \\ 0 \end{bmatrix} \quad \boldsymbol{x}_{0} = \begin{bmatrix} -10 \\ 0 \\ 1 \\ 0 \\ 20n \\ 0 \end{bmatrix}$$

Here, $n = 1.06 \times 10^{-3}$ rad/s is the reference orbit's mean motion. Based on these choices, the first receiver is actually the reference point, whereas the other receivers are moving relative to the reference orbit.

TDOA measurements are collected at the initial time $t_1 = t_0 = 0$ and $t_2 = 992.31$ s. The measurements are simulated by propagating the motion of the transmitter and receivers using Eq. (2). (Note that propagation of the transmitter's motion using Eq. (2) neglects dynamic modeling error.) Assume the TDOA measurements and receiver-location components each have standard deviations equal to $\sigma_{\Delta\rho} = \sigma_r = 1$ mm and all variables are uncorrelated.

$$\boldsymbol{P}_{\Delta\rho} = \sigma_{\Delta\rho}^2 \boldsymbol{I}_{6\times 6} \qquad \boldsymbol{P}_{j,k} = \sigma_r^2 \boldsymbol{I}_{3\times 3} \tag{33}$$

Based on an example draw from these error distributions, the resulting solutions for the transmitter position at the two measurement times are calculated using the method of [10] and are shown below.

$$\hat{\boldsymbol{r}}_1 = \begin{bmatrix} -10.0016724 \\ -0.0000763 \\ 1.0000797 \end{bmatrix} \text{km} \qquad \hat{\boldsymbol{r}}_2 = \begin{bmatrix} -4.9795330 \\ 17.2515739 \\ 0.4988957 \end{bmatrix} \text{km} \tag{34}$$

The resulting solution for the initial velocity is calculated using Eq. (6).

$$\hat{\boldsymbol{v}}_1 = \begin{bmatrix} 6.516 \times 10^{-5} \\ 0.02117443 \\ -1.401 \times 10^{-6} \end{bmatrix} \text{km/s} \tag{35}$$

The error in the transmitter initial state solution is summarized below, with units in km and km/s.

$$\delta\boldsymbol{x}_0 = \begin{bmatrix} -1.6724 \times 10^{-3} \\ -7.6285 \times 10^{-5} \\ 7.9716 \times 10^{-5} \\ 6.516 \times 10^{-5} \\ -3.030 \times 10^{-5} \\ -1.401 \times 10^{-6} \end{bmatrix} \tag{36}$$

Based on the error parameters and receiver locations, the components of the transmitter initial state covariance $\boldsymbol{P}_0$ are computed from Eq. (17) and are shown below.

$$\boldsymbol{P}_{rr} = \begin{bmatrix} 2.997 \times 10^{-5} & 1.421 \times 10^{-6} & -1.808 \times 10^{-6} \\ 1.421 \times 10^{-6} & 6.768 \times 10^{-8} & -8.582 \times 10^{-8} \\ -1.808 \times 10^{-6} & -8.582 \times 10^{-8} & 1.093 \times 10^{-7} \end{bmatrix} \text{km}^2 \tag{37}$$

$$\boldsymbol{P}_{vv} = \begin{bmatrix} 2.594 \times 10^{-9} & -1.251 \times 10^{-9} & -5.374 \times 10^{-11} \\ 1.251 \times 10^{-9} & 7.330 \times 10^{-10} & 2.558 \times 10^{-11} \\ -5.374 \times 10^{-11} & 2.558 \times 10^{-11} & 1.120 \times 10^{-12} \end{bmatrix} \text{km}^2/\text{s}^2 \tag{38}$$

$$\boldsymbol{P}_{rv} = \begin{bmatrix} -4.563 \times 10^{-8} & -3.955 \times 10^{-8} & 1.101 \times 10^{-9} \\ -2.164 \times 10^{-9} & -1.876 \times 10^{-9} & 5.229 \times 10^{-11} \\ 2.752 \times 10^{-9} & 2.385 \times 10^{-9} & -6.662 \times 10^{-11} \end{bmatrix} \text{km}^2/\text{s} \tag{39}$$

The bias of the transmitter initial state is computed from Eq. (28) and is shown below, in units of km and km/s.

$$\boldsymbol{b}_0 = \begin{bmatrix} -4.369 \times 10^{-6} \\ -2.059 \times 10^{-7} \\ 2.642 \times 10^{-7} \\ -1.985 \times 10^{-7} \\ 1.124 \times 10^{-7} \\ 4.077 \times 10^{-9} \end{bmatrix} \tag{40}$$

As mentioned in Section 5, the covariance and bias are functions of the transmitter initial state. Here, the true transmitter initial state was used to evaluate these quantities. In a real world application, the true transmitter initial state is unknown, and the computed estimate of the transmitter initial state would need to be used instead. Comparing the solution in Eqs. (34) and (35) with the true transmitter initial condition shows good agreement within the predicted covariance and bias.

The analytical predictions of the covariance and bias are further validated by Monte Carlo simulation. For this simulation 10 million trials were performed, taking random draws for the TDOA-measurement and receiver location error from zero-mean, Gaussian distributions with the described standard deviations. Using the initial conditions in Eq. (32), the components of the sample covariance for the population of transmitter initial state solutions are shown below.

$$\boldsymbol{P}_{rr} = \begin{bmatrix} 2.998 \times 10^{-5} & 1.421 \times 10^{-6} & -1.808 \times 10^{-6} \\ 1.421 \times 10^{-6} & 6.769 \times 10^{-8} & -8.584 \times 10^{-8} \\ -1.808 \times 10^{-6} & -8.584 \times 10^{-8} & 1.094 \times 10^{-7} \end{bmatrix} \text{km}^2 \tag{41}$$

$$\boldsymbol{P}_{vv} = \begin{bmatrix} 2.597 \times 10^{-9} & -1.252 \times 10^{-9} & -5.380 \times 10^{-11} \\ 1.252 \times 10^{-9} & 7.333 \times 10^{-10} & 2.560 \times 10^{-11} \\ 5.380 \times 10^{-11} & 2.560 \times 10^{-11} & 1.121 \times 10^{-12} \end{bmatrix} \text{km}^2/\text{s}^2 \tag{42}$$

$$\boldsymbol{P}_{rv} = \begin{bmatrix} -4.580 \times 10^{-8} & -3.947 \times 10^{-8} & 1.105 \times 10^{-9} \\ -2.172 \times 10^{-9} & -1.872 \times 10^{-9} & 5.246 \times 10^{-11} \\ 2.763 \times 10^{-9} & 2.381 \times 10^{-9} & -6.684 \times 10^{-11} \end{bmatrix} \text{km}^2/\text{s} \tag{43}$$

The sample bias for the population of transmitter initial state solutions is shown below, in units of km and km/s.

$$\boldsymbol{b}_0 = \begin{bmatrix} -4.035 \times 10^{-6} \\ -1.955 \times 10^{-7} \\ 2.449 \times 10^{-7} \\ -2.127 \times 10^{-7} \\ 1.190 \times 10^{-7} \\ 4.415 \times 10^{-9} \end{bmatrix} \tag{44}$$

These sample covariance and bias values show good agreement with the analytical predictions.

Two-Receiver Example

Consider the identical reference orbit as the previous example, and the initial states of two receivers and the transmitter, in units of km and km/s, are shown below.

$$\boldsymbol{x}_{A,0} = \begin{bmatrix} 0 \\ 0 \\ 0 \\ 0 \\ 0 \\ 0 \end{bmatrix} \quad \boldsymbol{x}_{B,0} = \begin{bmatrix} 1 \\ 0 \\ 0.1 \\ 0 \\ 0 \\ 0 \end{bmatrix} \quad \boldsymbol{x}_0 = \begin{bmatrix} -10 \\ 0 \\ 1 \\ 0 \\ 20n \\ 0 \end{bmatrix} \tag{45}$$

Six TDOA measurements are collected at time intervals of $\Delta t = 992.31$ s. Assume the TDOA measurements and receiver-location components each have standard deviations of $\sigma_{\Delta\rho} = 30$ cm and $\sigma_r = 10$ cm and all variables are uncorrelated. Based on an example draw from these error distributions, the resulting solution for the transmitter initial condition is obtained using Bertini and shown below, in units of km and km/s.

$$\hat{\boldsymbol{x}}_0 = \begin{bmatrix} -9.9992 \\ 0.001371 \\ 0.9910 \\ 2.2471 \times 10^{-7} \\ 0.021105 \\ -5.4723 \times 10^{-5} \end{bmatrix} \tag{46}$$

Relative to the true value, the associated errors are shown below.

$$\delta\boldsymbol{x}_0 = \begin{bmatrix} 7.6793 \times 10^{-4} \\ 1.3708 \times 10^{-3} \\ -9.0203 \times 10^{-3} \\ 2.2471 \times 10^{-7} \\ -1.4880 \times 10^{-6} \\ -5.4723 \times 10^{-5} \end{bmatrix} \tag{47}$$

Based on these parameters and receiver locations, the components of the transmitter initial state covariance $\boldsymbol{P}_0$ are computed from Eq. (17) and are shown below.

$$\boldsymbol{P}_{rr} = \tag{48}$$
$$\begin{bmatrix} 2.406 \times 10^{-6} & 4.362 \times 10^{-6} & -2.454 \times 10^{-5} \\ 4.362 \times 10^{-6} & 3.170 \times 10^{-5} & -1.357 \times 10^{-5} \\ -2.454 \times 10^{-5} & -1.357 \times 10^{-5} & 3.455 \times 10^{-4} \end{bmatrix} \text{km}^2$$

$$\boldsymbol{P}_{vv} = \tag{49}$$
$$\begin{bmatrix} 3.428 \times 10^{-13} & -1.192 \times 10^{-12} & 5.679 \times 10^{-12} \\ -1.192 \times 10^{-12} & 9.018 \times 10^{-12} & -6.175 \times 10^{-12} \\ 5.679 \times 10^{-12} & -6.175 \times 10^{-12} & 1.531 \times 10^{-9} \end{bmatrix} \text{km}^2/\text{s}^2$$

$$\boldsymbol{P}_{rv} = \tag{50}$$
$$\begin{bmatrix} 6.667 \times 10^{-10} & -4.642 \times 10^{-9} & 4.648 \times 10^{-9} \\ 3.076 \times 10^{-9} & -7.201 \times 10^{-9} & 5.947 \times 10^{-8} \\ -4.812 \times 10^{-9} & 4.894 \times 10^{-8} & -3.130 \times 10^{-8} \end{bmatrix} \text{km}^2/\text{s}$$

The bias of the transmitter initial state solution is computed from Eq. (28) and is shown below, in units of km and km/s.

$$\boldsymbol{b}_0 = \begin{bmatrix} -3.088 \times 10^{-5} \\ -1.028 \times 10^{-4} \\ -8.359 \times 10^{-5} \\ -8.938 \times 10^{-9} \\ 5.703 \times 10^{-8} \\ 4.802 \times 10^{-7} \end{bmatrix} \tag{51}$$

Comparing the solution in Eq. (46) with the true transmitter initial condition shows good agreement within the predicted covariance and bias.

The analytical predictions of the covariance and bias are further validated by Monte Carlo simulation. Ten million trials were performed, taking random draws for the TDOA-measurement and recevier location error from zero-mean, Gaussian distributions with standard deviations given in Eq. (33). Newton's method was used to solve the system of polynomials for the Monte Carlo simulations as it was orders of magnitude faster than Bertini. The initial guess required for Newton's method was the nominal state of the transmitter, which was known for the Monte Carlo simulations. In reality having a sufficient initial guess is not likely, so a method like Bertini must be used to determine the transmitter state. Using the initial conditions in Eq. (45), the components of the sample covariance for the population of transmitter initial state covariance are shown below.

$$\boldsymbol{P}_{rr} = \tag{52}$$
$$\begin{bmatrix} 2.406 \times 10^{-6} & 4.363 \times 10^{-6} & -2.451 \times 10^{-5} \\ 4.363 \times 10^{-6} & 3.172 \times 10^{-5} & -1.349 \times 10^{-5} \\ -2.451 \times 10^{-5} & -1.349 \times 10^{-5} & 3.456 \times 10^{-4} \end{bmatrix} \text{km}^2$$

$$\boldsymbol{P}_{vv} = \tag{53}$$
$$\begin{bmatrix} 3.429 \times 10^{-13} & -1.192 \times 10^{-12} & 5.652 \times 10^{-12} \\ -1.192 \times 10^{-12} & 9.017 \times 10^{-12} & -6.021 \times 10^{-12} \\ 5.652 \times 10^{-12} & -6.021 \times 10^{-12} & 1.536 \times 10^{-9} \end{bmatrix} \text{km}^2/\text{s}^2$$

$$\boldsymbol{P}_{rv} = \tag{54}$$
$$\begin{bmatrix} 6.667 \times 10^{-10} & -4.642 \times 10^{-9} & 4.562 \times 10^{-9} \\ 3.078 \times 10^{-9} & -7.202 \times 10^{-9} & 5.907 \times 10^{-8} \\ -4.805 \times 10^{-9} & 4.890 \times 10^{-8} & -3.172 \times 10^{-8} \end{bmatrix} \text{km}^2/\text{s}$$

The sample bias for the population of transmitter initial state solutions is shown below, in units of km and km/s.

$$\boldsymbol{b}_0 = \begin{bmatrix} -3.045 \times 10^{-5} \\ -1.021 \times 10^{-4} \\ -9.023 \times 10^{-5} \\ -8.813 \times 10^{-9} \\ 5.621 \times 10^{-8} \\ 5.032 \times 10^{-7} \end{bmatrix} \tag{55}$$

These sample covariance and bias values show good agreement with the analytical predictions.

7. CONCLUSIONS

Whereas TDOA measurements, perhaps collected by space-based receivers, have been largely studied for the geolocation of an Earth-fixed transmitter, the solutions presented here consider the use of TDOA for initial orbit determination. The description of the solution accuracy with respect to TDOA measurement errors and receiver position errors allows analysis of the feasibility of the orbit-determination solution given error specifications. The solutions presented here reduce the problem to solving a system of six quadratic equations (for two or three receivers) or solving two systems of three quadratic equations followed by a system of three linear equations (for four receivers). The method allows the orbit determination of an active satellite transmitting at a particular frequency. TDOA orbit determination does not depend on lighting conditions as is encountered when using optical sensors. Also, TDOA orbit determination could potentially utilize low-gain antennas that do not require a priori knowledge to cue the receiver pointing.

REFERENCES

[1] K. Ho and Y. Chan, "Solution and performance analysis of geolocation by TDOA," *IEEE Transactions on Aerospace and Electronic Systems*, vol. 29, no. 4, pp. 1311–1322, 1993.

[2] Y. Chan and K. Ho, "A simple and efficient estimator for hyperbolic location," *IEEE Transactions on Signal Processing*, vol. 42, no. 8, pp. 1905–1915, 1994.

[3] K. C. Ho and Y. T. Chan, "Geolocation of a known altitude object from TDOA and FDOA measurements," *IEEE Transactions on Aerospace and Electronic Systems*, vol. 33, no. 3, 1997.

[4] N. Levanon, "Quick position determination using 1 or 2 LEO satellites," *IEEE Transactions on Aerospace and Electronic Systems*, vol. 34, no. 3, pp. 736–754, 1998.

[5] T. Pattison and S. I. Chou, "Sensitivity analysis of dual-satellite geolocation," *IEEE Transactions on Aerospace and Electronic Systems*, vol. 36, no. 1, pp. 56–71, 2000.

[6] J. Mason, "Algebraic two-satellite TOA/FOA position solution on an ellipsoidal earth," *IEEE Transactions on Aerospace and Electronic Systems*, vol. 40, no. 3, pp. 1087–1092, 2004.

[7] J. Mason and L. Romero, "TOA/FOA geolocation solutions using multivariate resultants," *Navigation*, vol. 52, no. 3, pp. 163–177, 2005.

[8] L. A. Romero and J. Mason, "Evaluation of direct and iterative methods for overdetermined systems of TOA geolocation equations," *IEEE Transactions on Aerospace and Electronic Systems*, vol. 47, no. 2, pp. 1213–1229, 2011.

[9] ——, "Geolocation using TOA, FOA, and altitude information at singular geometries," *IEEE Transactions on Aerospace and Electronic Systems*, vol. 51, no. 2, pp. 1069–1078, 2015.

[10] A. J. Sinclair, T. A. Lovell, and J. Darling, "RF localization solution using heterogeneous TDOA," in *IEEE Aerospace Conference*, Big Sky, Montana, March 2015.

[11] J. P. DeVries, "Elliptic elements in terms of small increments of position and velocity components," *AIAA Journal*, vol. 1, no. 11, pp. 2626–2629, 1963.

[12] W. H. Clohessy and R. S. Wiltshire, "Terminal guidance system for satellite rendezvous," *Journal of the Aerospace Sciences*, vol. 27, no. 9, pp. 653–658, 1960.

[13] J. Tschauner and P. Hempel, "Rendezvous zu einem in elliptischer bahn umlaufenden ziel," *Astronautica Acta*, vol. 11, no. 2, pp. 104–109, 1965.

[14] K. Yamanaka and F. Ankersen, "New state transition matrix for relative motion on an arbitrary elliptical orbit," *Journal of Guidance, Control, and Dynamics*, vol. 25, no. 1, pp. 60–66, 2002.

[15] A. J. Sinclair, R. E. Sherrill, and T. A. Lovell, "Geometric interpretation of the tschauner-hempel solutions for satellite relative motion," *Advances in Space Research*, 2015, doi: http://dx.doi.org/10.1016/j.asr.2015.01.032.

[16] D. J. Bates, J. D. Hauenstein, A. J. Sommese, and C. W. Wampler, *Numerically Solving Polynomial Systems with Bertini*. SIAM, Philadelphia, 2013.

BIOGRAPHY

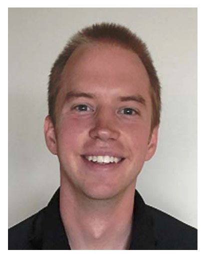

Simon Shuster *is a Master's student in Aerospace Engineering at Utah State University under David Geller. He spend the summer of 2016 at AFRL working on space-based RF localization. He received a Bachelor of Aerospace Engineering and Mechanics from the University of Minnesota in 2014. His research interests include astrodynamics and spacecraft navigation.*

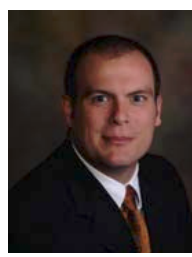

Andrew J. Sinclair *is a Senior Aerospace Engineer in the Space Vehicles Directorate of the Air Force Research Laboratory. He received B.S. and M.S. degrees in aerospace engineering from the University of Florida in 2000 & 2001, and a Ph.D. in aerospace engineering from Texas A&M University in 2005. From 2005 to 2016, he was a faculty member in Aerospace Engineering at Auburn University. His current research interests include dynamics, navigation, and control for spacecraft formation flight.*

T. Alan Lovell *is a Research Aerospace Engineer in the Space Vehicles Directorate of the Air Force Research Laboratory (U.S.). He received his B.S. from Georgia Tech in 1991, his M.S. from Arizona State University in 1994, and his Ph.D. from Auburn University in 2001; all three degrees are in Aerospace Engineering. He has authored or coauthored over 100 conference papers and 30 journal articles on Astrodynamics and Spacecraft Guidance, Navigation, and Control. He is an Associate Fellow of of AIAA. His research interests include astrodynamics, orbit determination, trajectory optimization, and feedback control design.*